RE.PUBLIC@POLIMI
Research Publications at Politecnico di Milano

Post-Print

This is the accepted version of:

H.C. Henninger, J.D. Biggs
Near Time-Minimal Earth to L1 Transfers for Low-Thrust Spacecraft
Journal of Guidance Control and Dynamics, Vol. 40, N. 11, 2017, p. 2994-2999
doi:10.2514/1.G002373

The final publication is available at https://doi.org/10.2514/1.G002373

Access to the published version may require subscription.

When citing this work, cite the original published paper.

Permanent link to this version
http://hdl.handle.net/11311/1043411

Near Time-Minimal Earth to L_1 Transfers for Low-Thrust Spacecraft

Helen C. Henninger [⋆], James D. Biggs[a]

Politecnico di Milano, Via La Masa 34 - 20156 Milano, Italy

1 Introduction

Time- and propellant- optimal Earth-Moon transfers and transfers to orbits of the Earth-Moon L_1-point using electric propulsion are well-studied [1–5]; a common method is to employ Pontryagin's maximum principle, [6] which provides necessary conditions for optimality in the form of a dynamical system of state and co-state equations with a set of boundary conditions. A potential way of solving such boundary value problems is via an indirect shooting method [7, 8]. However, in the elliptic domain (specific orbital energy is strictly less than zero), the low thrust of electrical propulsion means that the satellite motion is a perturbation of a conservative system admitting periodic and quasi-periodic trajectories. This makes it possible to select coordinates such that the satellite dynamics has a fast and slow component (i.e. components develop in different time scales) [9]. Due to these two time scales, the shooting method is not robust over the whole trajectory: the fast time scale introduces rapid oscillations into the time integral of the dynamics, which in turn introduces multiple local solutions which can prohibit convergence to the global minima [10]. Averaging with respect to the fast variable is a classical technique for treating these systems [11–13]. This eliminates the fast variable and so increases the robustness of the numerical method. However, while averaging is valid for transfers between orbits around Earth, when designing Earth-Moon or Earth-Moon L_1 halo orbit transfers, it is essential to identify the region where the thrust becomes significantly large enough that the assumption that satellite motion is a perturbation of a conservative system is no longer valid. Averaging must be "switched off" beyond this point for the sake of accuracy.

Previous studies of such interplanetary transfers have used multiple distinct arcs; the patched-conic method is a classical example of this approach which uses high-thrust and a delta-v maneuver to cancel the hyperbolic excess velocity upon Moon arrival. Other low-thrust patching methods have been computed [14–16]; but often also require a delta-v at the point where the two trajectories are patched to match the energies. We devise a method that separates an Earth-L_1 trajectory into two arcs and uses three steps to solve a minimum-time transfer with continuous thrust by (i) Averaging the necessary conditions for optimal-

⋆Postdoctoral researcher, Dipartimento di Scienze e Tecnologie Aerospaziale, Via Arpesani 8, 20139, Milano, Italy, helenclare.henninger@polimi.it

[a]Professor, Dipartimento di Scienze e Tecnologie Aerospaziale, Via La Masa 34 - 20156 Milano, Italy, jamesdouglas.biggs@polimi.it

ity and using numerical shooting to solving a minimum-time transfer from near-Earth orbit to the boundary of the region where averaging is applicable. (ii) Solving a minimum-time transfer without averaging using numerical shooting from this orbit to the Earth-Moon Lagrange point L_1 (since two possible interplanetary missions with initial near-Earth orbits are to the Moon or a libration point orbit and an optimal continuous-thrust Earth- Moon transfer generally bypasses L_1 quite closely, such a mission demonstrates both possibilities). These two steps yield two trajectories (in state and costate variables) that are minimum-time individually (only in the average sense for step (i)), but the concatenation of the two has a discontinuity in the state and costate space and carries no extremality property. (iii) A third combined problem is solved where the shooting equation is constructed to ensure the two extremal trajectories in steps (i) and (ii) join continuously in the state and costate, which restores the extremality of the transfer. The arcs join smoothly with no delta-V required to match the specific orbital energy. Constructing and demonstrating this method of patching averaged and non-averaged trajectories in an extremality preserving way is the main contribution of this Note. Furthermore, since we consider the case where the low-thrust propulsion is continuous way, these time-minimizing transfers are also propellant- minimizing transfers.

2 EARTH-TO-L_1 TRANSFER

This section describes the two minimum-time problems constructed in steps (i) and (ii) and the problem (iii) which is constructed to ensure that the two extremal trajectories of the subproblems (i) and (ii) join in an optimal way. Section 2.1 recalls the dynamics of the satellite in the Earth-centered motion under the influence of Sun and Moon gravity; the numerical averaging method is presented, and the shooting equation used in step (i) is constructed. Section 2.2 reviews the synodic bicircular four-body problem and the shooting equation used in step (ii) is constructed. Section 2.3. describes the shooting conditions of the third step of the transfer and the construction of the third shooting equation.

2.1 Subproblem 1: Averaged Earth-Centered Problem This subproblem solves the minimum-time problem *with averaging* from the initial orbit about Earth to an orbit of radius R_f in Earth-centered motion under the influence of Moon and Sun gravity. The dynamics are expressed in in modified standard orbital elements $\mathbf{x} = (p, e_x, e_y, \ell)$ in the earth-centered frame. These elements are used rather than the Kepler elements $a, e, \omega, \ell)$ so that they are defined for circular orbits. The satellite dynamics are given by the Gauss equations and the variable ℓ is the fast variable, and $\mathbf{x} = (p, e_x, e_y)$ are the slow variables. The thrust magnitude $\|\mathbf{u}\|$ is assumed to be constant and the satellite is fully-actuated.

The target radius R_f is chosen such that the 'thrust ratio' $\frac{\|\mathbf{u}\|\, r^2(t)}{\mu_E\, m}$ [17] (where μ_E is the Earth standard gravitational parameter, m is the satellite mass and $\|\mathbf{u}\|$ is the satellite thrust magnitude) remains lower than the value $\epsilon_{\text{ratio}} = 0.0004$ ([17] uses $\epsilon_{\text{ratio}} = 0.001$) throughout the transfer, i.e. $R_f = \frac{\mu_E\, m\, \epsilon_{\text{ratio}}}{\|\mathbf{u}\|}$. The satellite parameters used in both this subproblem and subproblem 2 are given in table 1 and the initial satellite orbit is given by $p^0 = 1.9 \times 10^4 km$, $e_x^0 = 0.1$, $e_y^0 = 0$, $i^0 = 0$ rad, $\ell^0 = 0$ rad, the final time guess is $3.864154 \times 10^4 s$ and the epoch of departure is 15 May 2014, at 3:35 UCT. The thrust magnitude $\|\mathbf{u}\|$ is assumed to be constant. Fig.1 shows the positions of the Earth, Sun, Moon and satellite at epoch for this transfer: that is, the Earth and Moon are located at angular position α_M^0, α_S^0, their epoch angular positions.

Table 1: Numerical parameters of model satellite

Satellite parameters :	Value:
$\|\mathbf{u}\|$	$3.75 \times 10^{-3}\ N$
Specific impulse I_0	$9000\ s$
Mass m	$5\ kg$
Thrust/mass ratio	$7.5 \times 10^{-4}\ m \cdot s^{-2}$

Table 2 lists the electric propulsion methods available for microsatellites. Of those available, for the example mission we compute, FEEP is the most suitable propulsion.

Table 2: Summary of electric propulsion technologies available for microsatellites (c.f. [18, 19])

Thruster Type:	Thrust (mN):	I_{sp} (s):	Power (W):	Thruster mass (kg):
Hall/Ion	0.4 - 20	300-3700	14-300	≤ 1
FEEP/colloid	$0.1\mu N$ - 1.5	450-9000	1-100	0.1 - 1
Electromagnetic	0.03-2	200-4000	3-300	0.06 - 0.5
Indium FEEP	> 1	9000	80	0.1 - 1

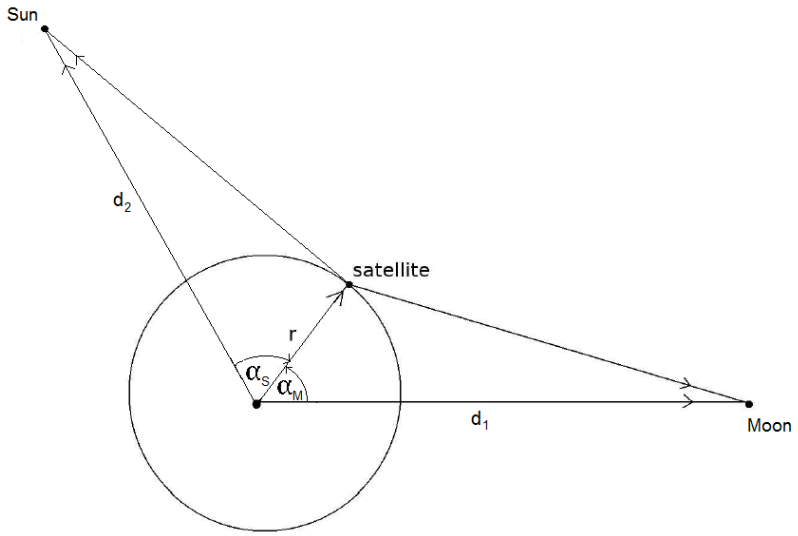

Figure 1: Configuration of Earth, satellite, Sun and Moon in subproblem 1

The Moon's (and Sun's) gravitational forces are included in the Gauss equations by decomposing them in the satellite radial-orthoradial frame; in the case of the Moon

$$u_{\text{Moon}} = \begin{bmatrix} \frac{-\mu_M}{r^2} + \frac{\mu_M}{\|d_1\|^2}\gamma_M \left(\left(-1 + \cos\alpha_M \frac{W}{1+\gamma_M W_M + \sqrt{1-\gamma_M W_M}}\right)\right) \\ \frac{\mu_M}{\|d_1\|^2}\gamma_M \left(-\sin\alpha_M \frac{W_M}{1+\gamma_M W_M + \sqrt{1-\gamma_M W}}\right) \end{bmatrix} \tag{1}$$

where μ_M is the standard gravitational parameter of the Moon, d_1 is the Earth-Moon distance and $\omega_M = \sqrt{\frac{\mu_E+\mu_M}{d_1^3}}$ is the angular speed of the Moon and the values γ_M, W_M are given in

$$\gamma_M = \frac{r}{\|d_1\|}, \quad \gamma_S = \frac{r}{\|d_2\|}, \quad (1 - 2\cos\alpha_M\gamma_M + \gamma_M^2)^3 = 1 - \gamma_M W_M, \quad (1 - 2\cos\alpha_S\gamma_S + \gamma_S^2)^3 = 1 - \gamma_S W_S. \tag{2}$$

The value $\alpha_M = \ell - \omega_M t - \alpha_M^0$ and $\alpha_S = \ell - \omega_S t - \alpha_S^0$. The decomposition of the Sun force is similar, except $\alpha_M, \mu_M, \gamma_M$ are replaced respectively by α_S, μ_S and γ_S, where μ_S is the standard gravitational parameter of the Sun, d_2 is the distance between the Sun and the Earth-Moon barycenter and $\omega_S = \frac{\mu_M+\mu_E+\mu_S}{d_2^2}$. The values γ_S and W_S are given in equation (2). Including these forces in the standard Gauss equations gives rise to the dynamics

$$\dot{\mathbf{x}} = G(\mathbf{x}, \ell, t)(\mathbf{u} + \mathbf{u}_{\text{Sun}} + \mathbf{u}_{\text{Moon}}), \quad \dot{\ell} = Q(\mathbf{x}, \ell), \quad \dot{m} = -\frac{\|\mathbf{u}\|}{g_0 I_{sp}} \tag{3}$$

where

$$G(\mathbf{x}, \ell, t) = \begin{bmatrix} 0 & \frac{2p\frac{p}{\mu_E}}{(1+e_y\cos\ell+e_x\sin\ell)M} \\ \frac{p}{\mu_E}\frac{\sin\ell}{M} & \frac{p}{\mu_E}\frac{e_x+\sin\ell(2+e_y\cos\ell+e_x\sin\ell)}{(1+e_y\cos\ell+e_x\sin\ell)M} \\ -\frac{p}{\mu_E}\frac{\cos\ell}{M} & \frac{p}{\mu_E}\frac{e_y+\cos\ell(2+e_y\cos\ell+e_x\sin\ell)}{(1+e_y\cos\ell+e_x\sin\ell)M} \end{bmatrix}, \quad Q(\mathbf{x}, \ell) = \frac{\sqrt{\mu_E}(1 + e_x\cos\ell + e_y\sin\ell)^2}{p^{3/2}}.$$

and g_0 is the Earth standard gravity.

The shooting function is now constructed. The boundary condition $r(\mathbf{x}(t_f^1), \ell(t_f^1)) = R_f$ is simplified by requiring that $e_x(t_f^1) = 0$, $e_y(t_f^1) = 0$, which removes dependence of this final condition on the fast variable ℓ (which unnecessarily increased the computation time). The Pontryagin's principle [6] associates to the problem of optimizing the trajectory of (3) with respect to time, the Hamiltonian function $\mathcal{H}_1(\mathbf{x}, \ell, \boldsymbol{\lambda}, \lambda_\ell, u, t) = G(\mathbf{x}, \ell, t)(\mathbf{u}_{\text{Sun}} + \mathbf{u}_{\text{Moon}}) + \boldsymbol{\lambda}(G(\mathbf{x}, \ell, t)\mathbf{u} + \lambda_\ell\, Q(\mathbf{x}, \ell) + \lambda_m\left(-\frac{\|\mathbf{u}\|}{g_0 I_{sp}}\right) - 1)$ and the Hamiltonian system

$$(\dot{\mathbf{x}}, \dot{\ell}, \dot{m}, \dot{\boldsymbol{\lambda}}, \dot{\lambda}_\ell, \dot{\lambda}_m) = J(\mathbf{x}, \ell, m, \boldsymbol{\lambda}, \lambda_\ell, \lambda_m, t) \tag{4}$$

where $\boldsymbol{\lambda}, \lambda_\ell, \lambda_m$ are the costate variables associated to $\mathbf{x}, \ell, m$. The transversality condition

$$\lambda_\ell(t_f^1) = 0, \tag{5}$$

also arises from the Pontryagin's principle, and the condition $\mathcal{H}_1(\mathbf{x}(t_f^1), \ell(t_f^1), m(t_f^1)m\boldsymbol{\lambda}(t_f^1), \lambda_\ell(t_f^1), \lambda_m(t_f^1), t_f^1) = 0$. This condition is replaced by the equivalent condition on the norm of the costate vector,

$$\|\boldsymbol{\lambda}^0\|^2 + (\lambda_\ell^0)^2 + (\lambda_m^0)^2 = 1. \tag{6}$$

Finally, since there is no final condition on the mass, the final value

$$\lambda_m(t_f^1) = 0. \tag{7}$$

Averaging with respect to the angular variable ℓ is applied numerically in the form of the Riemann sum

$$\mathcal{S}(\bar{\mathbf{x}}, \bar{m}, \bar{\ell}, \bar{\boldsymbol{\lambda}}, \bar{\lambda}_\ell, \bar{\lambda}_m, t) = \sum_{i=1}^{\mathrm{n_{av}}} \frac{J(\mathbf{x}, \ell, m, \boldsymbol{\lambda}, \lambda_\ell, \lambda_m, t)}{Q(\mathbf{x}, \ell_i^*)} \frac{2\pi}{\mathrm{n_{av}}}, \quad \ell_{i-1} \leq \ell_i^* \leq \ell_i, \tag{8}$$

where $\bar{\cdot}$ denotes the average variable, $\ell \in I = [0, 2\pi]$, $\ell_i^* = i \times \frac{2\pi}{\mathrm{n_{av}}}$ and the partition of I is

$$\text{Part} = \left\{ \left[0, \frac{2\pi}{\mathrm{n_{av}}}\right], \left[2\frac{2\pi}{\mathrm{n_{av}}}, 3\frac{2\pi}{\mathrm{n_{av}}}\right], \ldots, \left[(\mathrm{n_{av}} - 1)\frac{2\pi}{\mathrm{n_{av}}}, 2\pi\right] \right\}.$$

The averaged dynamics are denoted by

$$(\dot{\bar{\mathbf{x}}}, \dot{\bar{\ell}}, \dot{\bar{m}}, \dot{\bar{\boldsymbol{\lambda}}}, \dot{\bar{\lambda}}_\ell, \dot{\bar{\lambda}}_m) = \mathcal{S}(\bar{\mathbf{x}}, \bar{m}, \bar{\ell}, \bar{\boldsymbol{\lambda}}, \bar{\lambda}_\ell, \bar{\lambda}_m, t). \tag{9}$$

Since the summand in (8) depends on time, we may average with "constant time" in the Riemann sum (8), or notice that the time t is a function of the angular variable, $t(\ell)$ which would give rise to an "averaged time" $\bar{t}$. While using "averaged time" is more realistic since the gravitational forces due to the Sun and Moon are time-varying, maintaining time as an independent variable and ℓ as a state variable - as done in (8) - simplifies the construction of the canonical transformation mapping non-averaged to averaged variables, which will be applied in the third shooting (subsection 2.3).

The boundary conditions $r(\mathbf{x}(t_f^1), \ell(t_f^1), m(t_f^1)) = R_f$, (5) and (6) and (7) are expressed in terms of averaged variable and used to construct the shooting function

$$S^1 : (t_f^1, \bar{\boldsymbol{\lambda}}^0, \bar{\lambda}_\ell^0, \bar{\lambda}_m^0) \mapsto \begin{bmatrix} \bar{a}^f - R_f \\ \bar{e}_x^f \\ \bar{e}_y^f \\ \bar{\lambda_m}^f \\ \bar{\lambda_\ell}^f \\ \|\bar{\boldsymbol{\lambda}}^0\|^2 + (\bar{\lambda}_\ell^0)^2 + (\bar{\lambda}_m^0)^2 - 1 \end{bmatrix}. \tag{10}$$

Solving the shooting equation $S^1(t_f^1, \bar{\boldsymbol{\lambda}}^0, \bar{\lambda}_\ell^0, \bar{\lambda}_m^0) = 0$ numerically gives the initial costate vector $(\bar{\lambda}^0, \bar{\lambda}_\ell^0, \bar{\lambda}_m^0)$ and the transfer time t_f^1 required to construct the extremal pair $(\bar{\mathbf{x}}(t), \bar{\ell}(t), \bar{\boldsymbol{\lambda}}(t), \bar{\lambda}(t))$. The specific orbital energy $-\mu_E/2a$ of the satellite at the final time t_f^1 and the final mass $m(t_f^1)$ are determined numerically and denoted by E_f, m_f respectively. A negative energy is expected since the satellite remains in the elliptic domain while $r(t) < R_f$.

2.2 Subproblem 2: Controlled Planar Restricted Four-Body Problem For the second step, four-body dynamics simplified using the bicircular assumptions of [20] and a planar assumption is used. Here, the three primaries are the Sun, Moon and Earth, and the simplifying hypotheses are

a) Two primaries (Earth and Moon) move in circular orbits around their mutual center of mass and are coplanar.

b) The third primary (Sun) is in circular orbit around the center of mass of the system formed by the first two primaries, and its orbit is coplanar with the orbits of those primaries.

Four-body motion is generally expressed using a standard normalization that fixes the Earth-Moon distance to 1. However, for the sake of consistency with the dynamics in subproblem 1, we will not normalize the variables. The dynamics are expressed in the synodic frame centered at the Earth-Moon barycenter and rotating with the angular speed of the Moon, so the Moon position is constant; we denote by c_1 the distance of the Earth from the Earth-Moon barycenter and c_2 the distance of the Moon from the Earth-Moon barycenter. The satellite coordinates in this frame are denoted by (X, Y). The dynamics are then

$$\begin{aligned} \ddot{X} &= 2\omega_M \dot{Y} + \omega_M^2 X + \tfrac{\mu_S}{A_S^3} - \mu_E \tfrac{X+X_M}{r_1^2} - \mu_M \tfrac{X-X_E}{r_2^3} - \mu_S \tfrac{X-X_S}{r_3^3} + u_1 \\ \ddot{Y} &= -2\omega_M \dot{X} + \omega_M^2 Y - \tfrac{\mu_S}{A_S^3} - \mu_E \tfrac{Y}{r_1^2} - \mu_M \tfrac{Y}{r_2^3} - \mu_S \tfrac{Y-Y_S}{r_3^3} + u_2 \end{aligned} \tag{11}$$

where

- $(X_E, Y_E) = (-c_1, 0)$ and $(X_M, Y_M) = (c_2, 0)$
- $(X_S, Y_S) = (d_2 \cos((t\omega_S - \omega_M) - \alpha_S^0), d_2 \sin((t\omega_S - \omega_M) - \alpha_S^0))$
- $r_1 = \sqrt{(X + c_1)^2 + Y^2}$
- $r_2 = \sqrt{(X - c_2)^2 + Y^2}$
- $r_3 = \sqrt{(X - X_S)^2 + (Y - Y_S)^2}$.

Denoting $(X, Y, \dot{X}, \dot{Y}) = (\xi_1, \xi_2, \xi_3, \xi_4)$, then the dynamics (11) have the form

$$\dot{\boldsymbol{\xi}} = P_0(\boldsymbol{\xi}) + \sum_{i=1}^{2} \boldsymbol{P}_i(\boldsymbol{\xi}) u_i. \tag{12}$$

and as in the previous subrproblem, $\dot{m} = -\frac{\|\mathbf{u}\|}{g_0 I_{sp}}$.

We now construct the shooting function. In the synodic frame, the specific orbital energy has the form

$$E(\boldsymbol{\xi}) = \frac{-\xi_3^2 - \xi_4^2 + (2\xi_2\xi_3 - 2(c + \xi_1)\xi_4)\omega_M - \left((c + \xi_1)^2 + \xi_2^2\right)\omega_M^2}{2} + \frac{\mu_E}{\sqrt{(c_1 + \xi_1)^2 + \xi_2^2}}. \tag{13}$$

Using the dynamics (12), we will perform a "backwards" shooting in minimum time to the specific orbital energy value E_f (determined numerically in the previous subproblem) *without averaging* (shooting *backwards* is achieved by changing lunar angular speed ω_M to $(-\omega_M)$ within this transfer.) The specific orbital energy value E_f is targeted rather than the radius R_f or Cartesian position, because if the target radius or position is reached with a positive energy, (on a hyperbolic or parabolic orbit), it may be impossible to find an initialization under which the costate vectors of subproblems 1 and 2 meet continuously in the third step, and due to the instability of the L_1-point, we are not guaranteed that the satellite will leave L_2 with a negative specific energy or that the energy will decrease to negative. Shooting backwards is necessary since, because of averaging, it is not possible to access to the angular variable $\ell(t_f^1)$ obtained in step 1. Thus we are unable to initialize a forward shooting from $x(t_f^1), \ell(t_f^1)$ to L_1 accurately. The boundary condition $m(t_f^2) = m_f$ is ndeeded so that the masses meet in step (iii). In order to obtain an initial value for m_0 at L_1, the transfer is initially performed with only the boundary condition $E(t_f^2) = E_f$, i.e. mass can develop freely. THe shooting is then carried out using the value m_0 which we deduce from the change in mass when it develops freely as the initial condition.

Denote $\boldsymbol{\xi}(\boldsymbol{\xi}^0, m^0, \boldsymbol{\Lambda}^0, \Lambda_m^0, t_f^2) = \boldsymbol{\xi}^f$ and $\boldsymbol{\Lambda}(\boldsymbol{\xi}^0, m^0, \boldsymbol{\Lambda}^0, \Lambda_m^0, t_f^2) = \Lambda^f$. The boundary conditions on mass and energy are expressed by $\mathcal{F}(\xi^f, m^f) = [E(\xi^f) - E_f, m^f = m_f]$. The transversality condition required by Pontryagin's principle has the form $\boldsymbol{\Lambda}^f \cdot d\mathcal{F}(\boldsymbol{\xi}^f) = 0$, and as in the previous section, the condition $\mathcal{H}_2(\boldsymbol{\xi}(t_f^2), m(t_f^2), \boldsymbol{\Lambda}(t_f^2), \Lambda_m(t_f^2)) = 0$ on the associated optimal Hamiltonian $\mathcal{H}_2 = \Lambda \cdot P_0(\boldsymbol{\xi}) + \|\mathbf{u}\| P_1(\boldsymbol{\xi}) \frac{\Lambda_3}{\sqrt{\Lambda_3^2+\Lambda_4^2}} + \|\mathbf{u}\| P_2(\boldsymbol{\xi}) \frac{\Lambda_4}{\sqrt{\Lambda_3^2+\Lambda_4^2}} + \Lambda_m \left(\frac{\|\mathbf{u}\|}{g_0 I_{sp}}\right)$ is replaced with the equivalent condition $\|\boldsymbol{\Lambda}^0\|^2 + (\Lambda_m^0)^2 = 1$. The shooting function is

$$S^2 : (t_f^2, \boldsymbol{\Lambda}^0, \Lambda_m^0) \mapsto \begin{bmatrix} E_f - E(\boldsymbol{\xi}^f) \\ m^f - m_f \\ [\boldsymbol{\Lambda}^f, \Lambda_m^f] \cdot d\mathcal{F}(\boldsymbol{\xi}^f, m^f) \\ \|\boldsymbol{\Lambda}^0\|^2 + (\Lambda_m^0)^2 - 1 \end{bmatrix}. \tag{14}$$

Solving the shooting equation $S^2(t_f^2, \boldsymbol{\Lambda}^0, \Lambda_m^0) = 0$ numerically gives the initial costate vector $[\boldsymbol{\Lambda}^0, \Lambda_m^0]$ required to construct the extremal pair $(\boldsymbol{\xi}(t), m(t), \boldsymbol{\Lambda}(t), \Lambda_m(t))$, and the transfer time t_f^2.

2.3 Joining the Extremal Pairs: The Combined Shooting Problem From the plot in Fig. 2 of the two extremal solutions obtained in subsections 2.1 and 2.2 in Cartesian coordinates, and the evolution of the separate orbital elements with respect to time, it is clear that there is a large discrepancy between the values $e_x(t_f^1), e_x(t_f^2)$ and $e_y(t_f^1), e_y(t_f^2)$; however, the value $a(t_f^1)$ joins $a(t_f^2)$ and $m(t_f^1)$ joins $m(t_f^2)$, which is expected, since the specific orbital energy depends only on the semi-major axis a (in the elliptic domain), and both transfers attain the same final specific orbital energy E_f and final mass m_f. These two arcs will now be joined smoothly. To do this, the initial costate vector $(\bar{\boldsymbol{\lambda}}^0, \bar{\lambda}_\ell^0, \bar{\lambda}_m^0, \boldsymbol{\Lambda}^0.\Lambda_m^0)$ and the two final times (t_f^1, t_f^2) are used as the guess to initialize a third shooting, where the shooting equation is constructed to ensure that the two extremal pairs of subproblems 1 and 2 join smoothly in the state and costate variables.

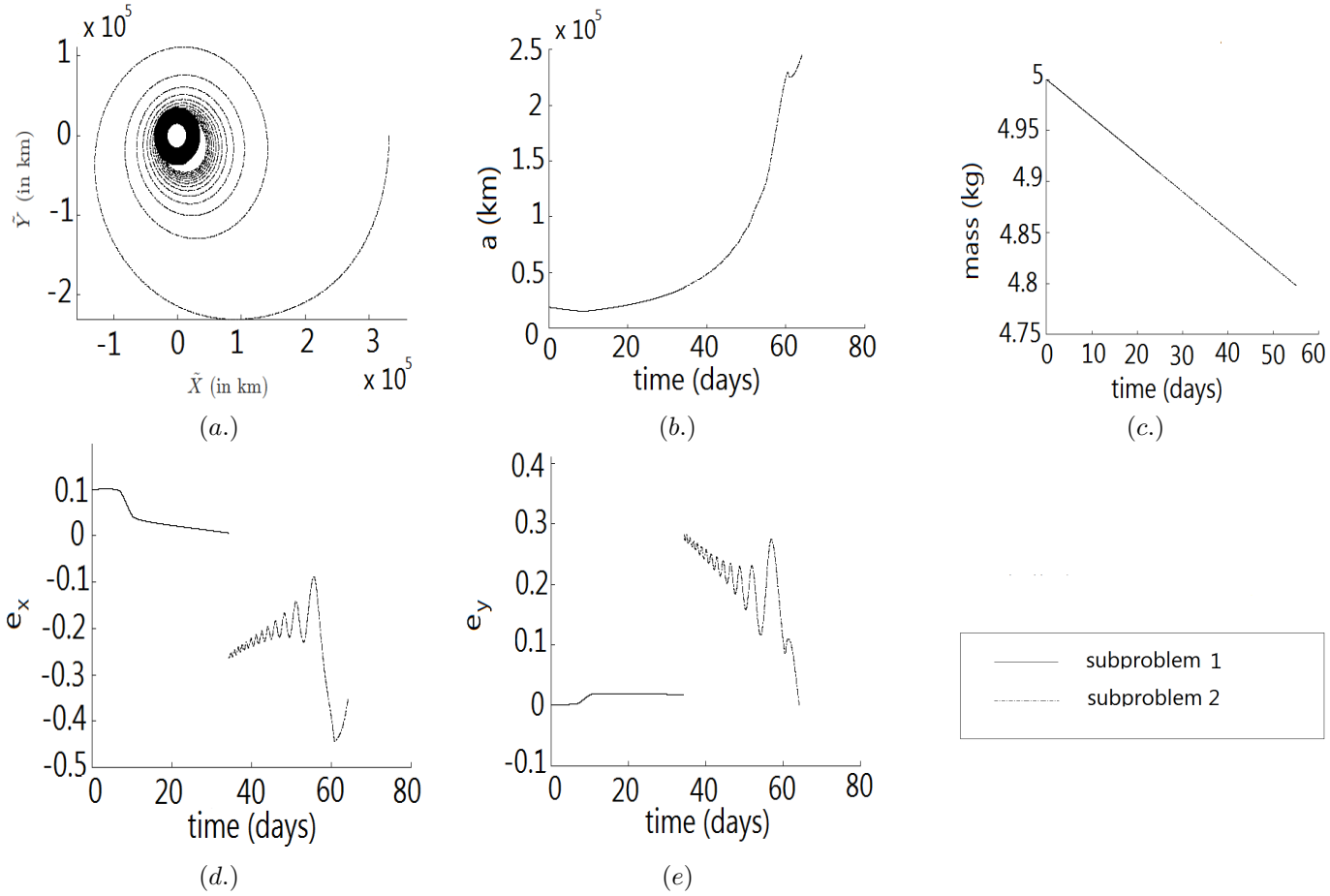

Figure 2: Trajectories of subproblems 1 & 2 a) in Cartesian coordinates b) Semimajor axis c) Mass d) e_x e) e_y

The transformation $\mathcal{T} : (\boldsymbol{\xi}, m, \boldsymbol{\Lambda}, \Lambda_m) \rightarrow (\bar{x}, \bar{\ell}, \bar{m}, \bar{\lambda}, \bar{\lambda}_\ell, \bar{\lambda}_m)$ is used to transform the non-averaged synodic curve $(\boldsymbol{\xi}(t), \boldsymbol{\Lambda}(t))$ obtained in the first subproblem to an averaged curve in the modified orbital elements. This transformation is constructed to be canonical so that the Hamiltonian system of the optimal problem is preserved. In constructing it, we make use of some simplifying assumptions about averaging with respect to the variable ℓ: firstly, that the average $\bar{\ell} = L$ (where L is the mean longitude), and secondly that the "slow" state variables $(\bar{p}, \bar{e}_x, \bar{e}_y) = (p, e_x, e_y)$ and $\bar{m} = m$. We then solve the ode

$$\begin{cases} \text{Dynamics :} \begin{cases} [\dot{\boldsymbol{\Lambda}}, \dot{\Lambda}_m] = -[\frac{\partial \mathcal{H}_2}{\partial \boldsymbol{\xi}}, \frac{\partial \mathcal{H}_2}{\partial m}] \\ \dot{\boldsymbol{\xi}} = P_0(\boldsymbol{\xi}) + \sum_{i=1}^{2} \boldsymbol{P}_i(\boldsymbol{\xi}) u_i \\ (\dot{\bar{\mathbf{x}}}, \dot{\bar{\ell}}, \dot{\bar{m}}, \dot{\bar{\boldsymbol{\lambda}}}, \dot{\bar{\lambda}}_\ell, \dot{\bar{\lambda}}_m) = \mathcal{S}(\bar{\mathbf{x}}, \bar{\ell}, \bar{m}, \bar{\boldsymbol{\lambda}}, \bar{\lambda}_\ell, \bar{\lambda}_m) \\ \dot{m} = -\frac{\|\mathbf{u}\|}{g_0 I_{sp}} \end{cases} \\ \text{Boundary conditions :} \begin{cases} \boldsymbol{\xi}^0 = (c_2, 0, 0, 0) \quad (L_1 \text{ position}) \\ (\mathbf{x}^0, \ell^0) = (1.9 \times 10^7, 0, 0, 0, 0) \quad (\text{Initial orbit}) \\ (\bar{\mathbf{x}}(t^*), \bar{\ell}(t^*), m(t^*), \bar{\boldsymbol{\lambda}}(t^*), \bar{\lambda}_\ell(t^*), \bar{\lambda}_m(t^*)) = \mathcal{T}(\boldsymbol{\xi}(t_f), m(t_f), \boldsymbol{\Lambda}(t_f), \Lambda_m(t_f)) \\ t = t^* + t_f, \quad \|\boldsymbol{\lambda}^0\|^2 + (\lambda_\ell^0)^2 + (\lambda_m^0)^2 = 1 \end{cases} \end{cases} \tag{15}$$

using the shooting method, where the shooting function is

$$S^3(t^*, T, \boldsymbol{\lambda}^0, \boldsymbol{\Lambda}^0) = \begin{bmatrix} \bar{\mathbf{x}}(t^*, \mathbf{x}^0, \ell^0, \lambda^0, \lambda_\ell^0) - \widetilde{\bar{\mathbf{x}}} \\ \bar{m}(t^*, \mathbf{x}^0, \ell^0, \lambda^0, \lambda_\ell^0) - \widetilde{m} \\ \text{mod}(\bar{\ell}(t^*, \mathbf{x}^0, \ell^0, \lambda^0, \lambda_\ell^0),\, 2\pi) - \text{mod}(\widetilde{\ell},\, 2\pi) \\ \bar{\lambda}(t^*, \mathbf{x}^0, \ell^0, \lambda^0, \lambda_\ell^0) - \widetilde{\bar{\lambda}} \\ \bar{\lambda}_\ell(t^*, \mathbf{x}^0, \ell^0, \lambda^0, \lambda_\ell^0) - \widetilde{\bar{\lambda}}_\ell \\ \bar{\lambda}_m(t^*, \mathbf{x}^0, \ell^0, \lambda^0, \lambda_\ell^0) - \widetilde{\bar{\lambda}}_m \\ \dfrac{\mu_E(-1 + \overline{e_x}^2 + \overline{e_y}^2)}{2\bar{p}} - E_f \\ \|\boldsymbol{\lambda}^0\|^2 + (\lambda_\ell^0)^2 + (\lambda_m^0)^2 - 1 \end{bmatrix} \tag{16}$$

(the notation $\text{mod}(\cdot,\, 2\pi)$ denotes the measure of the angle between 0 and 2π). Fig. 3 shows the result of this third shooting in the Cartesian coordinates and the corresponding development of the orbital elements. Here , there is a continuous join between the two arcs of the trajectory in each of the orbital elements a, e_x, e_y, mass m and ℓ (we do not show the plot of ℓ because the oscillations are so frequent from 0 to t_f that the plot is not very informative).

To demonstrate how closely the obtained trajectory in Fig 3 approximates a non-averaged extremal transfer (since the state and co-state variables are matched smoothly, this non-averaged solution will be a true extremal solution of the optimal control problem), in Fig. 4 we plot (in blue) the development of $\bar{a}, \overline{e_x}, \overline{e_y}$ for this transfer, while in red, we show the a, e_x, e_y

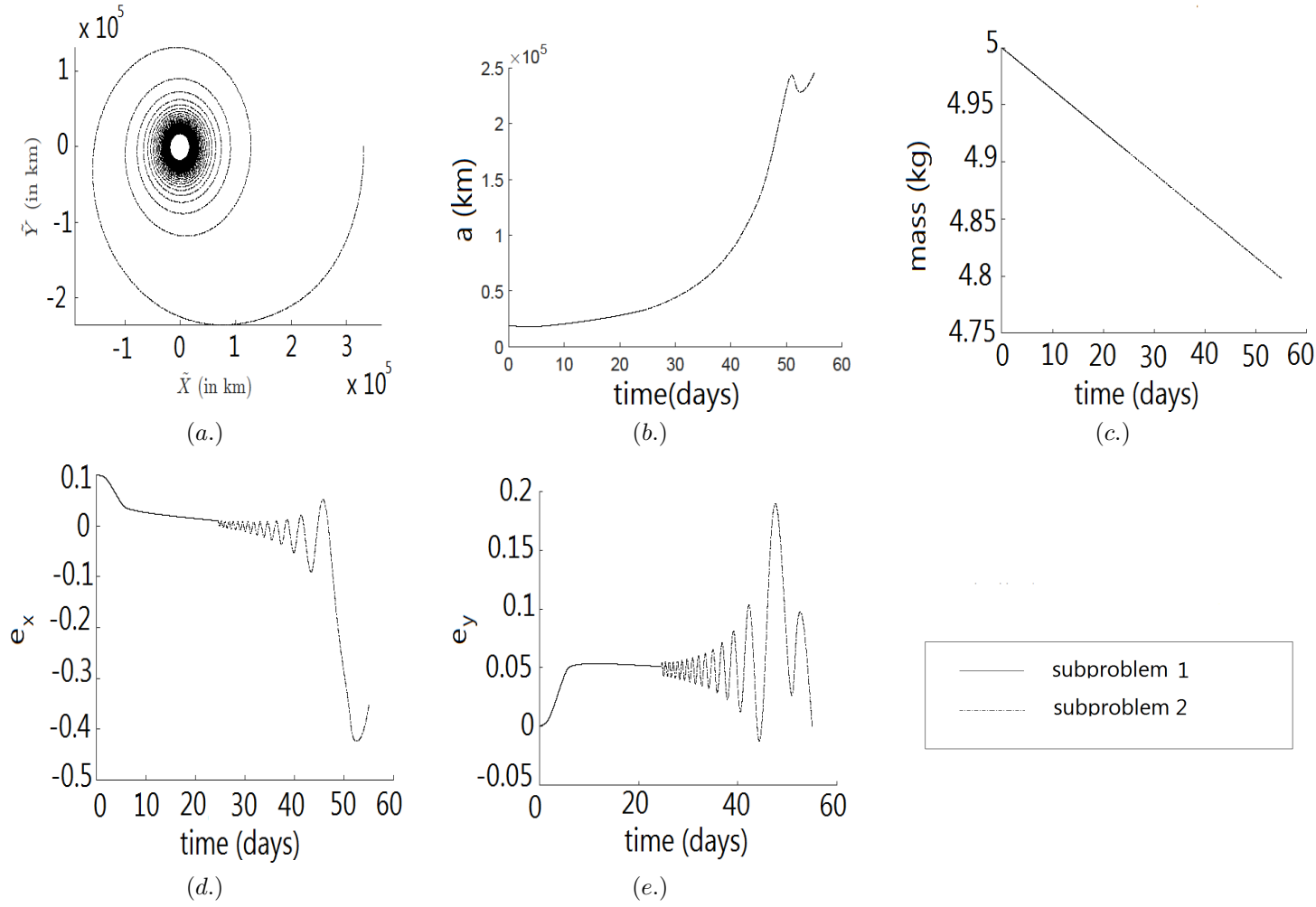

Figure 3: Solution of o.d.e in step (iii): a) Orbit in Cartesian coordinates b) Semimajor axis c) Mass d) e_x e) e_y

components for the solution of subproblem 3 where the averaged dynamics $(\dot{\bar{\mathbf{x}}}, \dot{\bar{\ell}}, \dot{\bar{m}}, \dot{\bar{\boldsymbol{\lambda}}}, \dot{\bar{\lambda}}_\ell, \dot{\bar{\lambda}}_m)$ in (15) are replaced with the non-averaged dynamics $(\dot{\mathbf{x}}, \dot{\ell}, \dot{m}, \dot{\boldsymbol{\lambda}}, \dot{\lambda}_\ell, \dot{\lambda}_m)$ given by (4) and the satellite parameters similarly come from table 1. We can gauge from this figure that the solution obtained via our method closely approximates the non-averaged extremal: the development of all variables follows the same scheme, and there is only a small time difference of 0.975 days between the two transfers.

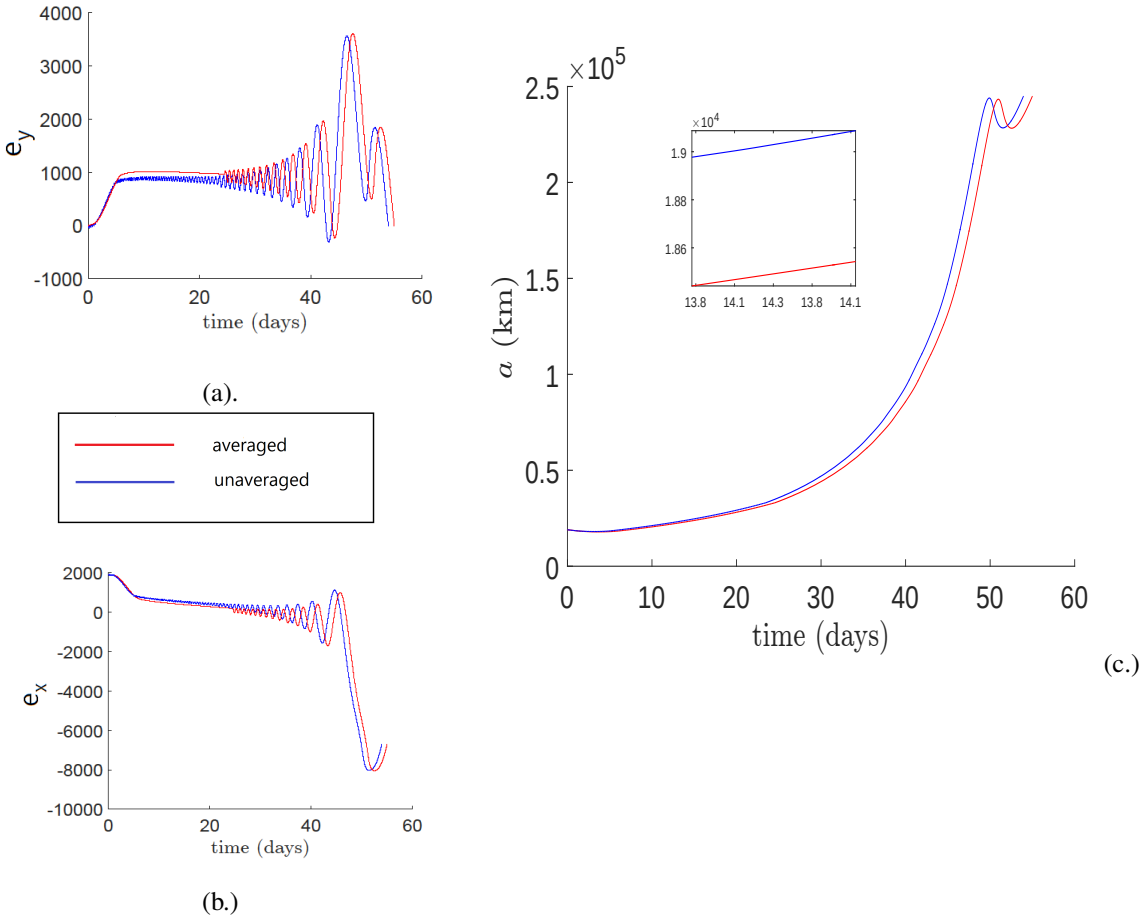

Figure 4: Development of components with and without averaging a) e_y b) e_x. c) Semimajor axis. Zoom shows oscillation in Kepler arc

3 CONCLUSION

Averaging is a well-known, widely-applied method to increase robustness in numerical computation of the solution of odes.However, this method cannot be applied to the equations of motion of low-thrust transfers leaving the near-earth region since the Earth gravity no longer dominates the thrust and so satellite motion can no longer be considered a perturbation of a conservative system admitting periodic and quasi-periodic trajectories. In these cases, patching of an averaged with a non-averaged trajectory can be applied, so that averaging is applied only over the near-earth region. When optimal trajectories are considered, matching the costates continuously between the patches is also required, to preserve extremality. In this Note, a time-optimal continuous, low-thrust transfer from the Earth to the Earth-Moon L_1-point was constructed using patching of an averaged and non-averaged arc where the costates as well as the states were matched smoothly to preserve extremality.

The method is demonstrated for a small satellite of mass $5kgs$ and acceleration $7.5 \times 10^{-4} m \cdot s^{-2}$. Comparing our patched, averaged trajectory with the true extremal trajectory (determined by turning off averaging on the first arc of the transfer, and using the averaged initial costate vector as an initial guess to compute the non-averaged extremal) shows that such a transfer has a time difference of 0.975 days with the true extremal. It can be inferred from this that extremality has been preserved after patching.

This method allows low-thrust extremal trajectories that leave the near-Earth region to be constructed where averaging increases the robustness of the computation over the full region where it is applicable. Such a method could be particularly useful for the mission analysis of extremal Earth-Moon trajectories, or trajectories to L_1 halo orbits, which which leave the near-Earth region and approach the L_1 point quite closely.

A limitation of this method (general to numerical shooting) is a high dependence on the initial guess. However, due to the increase in robustness, it was possible to initialize the costate variable by shooting on problems simpler than the actual one and using that initial costate vector as the first guess for the more complex problem. Making use of a global solver could further decrease this dependence. Including computation of eclipse duration and the J2-perturbation in the dynamics would also make this method more feasible, especially for analysis of CubeSat missions which are affected by perturbations and have a small battery capacity which requires limiting eclipse times. In this Note, the dynamics were restricted to the planar case to reduce the dimension of the problem, while demonstrating the concept; to increase applicability to real mission planning and analysis, the planar dynamics should be extended to a full three-dimensional model.

REFERENCES

[1] Casalino, L., Colasurdo, G., and Pastrone, D., "Optimal Low-Thrust Escape Trajectories Using Gravity Assist," *Journal of Guidance, Control, and Dynamics*, Vol. 22, No. 5, 1999, pp. 637-642. doi/pdf/10.2514/2.4451

[2] Herman, A. L., and B. A. Conway., "Optimal, Low-Thrust, Earth-Moon Orbit Transfer," *Journal of Guidance, Control, and Dynamics*, Vol. 21, No. 1, 1998, pp. 141-147. doi/pdf/10.2514/2.4210

[3] Ozimek, M. T., and K. C. Howell., "Low-Thrust Transfers in the Earth-Moon System, Including Applications to Libration Point Orbits," *Journal of Guidance, Control, and Dynamics*, Vol. 33, No. 2, 2010, pp. 533-549. doi/pdfplus/10.2514/1.43179

[4] Toputto, F., M. Vasile, and F. Bernelli-Zazzera, "Earth-to-Moon Low Energy Transfers Targeting L1 Hyperbolic Transit Orbits," *Annals of the New York Academy of Sciences*, Vol. 1065, No. 1, 2005, pp. 55-76. doi/10.1196/annals.1370.025/pdf

[5] Kluever, C. A., and B. L. Pierson, "Optimal low-thrust three-dimensional earth-moon trajectories," *Journal of Guidance, Control, and Dynamics*, Vol. 18, No. 4, 1995, pp. 830-837. doi/pdf/10.2514/3.21466

[6] Pontryagin, L. S., Boltyanskii, V.G., Gamkrelidze, R.V. and Mishchenko, E. F., *The Mathematical Theory of Optimal Processes, Translated from the Russian by K. N. Trirogoff, edited by L. W. Neustadt*, Interscience Publishers John Wiley & Sons, Inc., New York, 1962, pp. 17-21.

[7] Caillau, J-B., and B. Daoud, "Minimum Time Control of the Restricted Three-Body Problem," *SIAM Journal on Control and Optimization*, Vol. 50, No. 6, 2012, pp. 3178-3202. doi/pdf/10.1137/110847299

[8] Zhang, C., and Zhao, Y.-S., "Low-thrust Minimum-Fuel Optimization in the Circular Restricted Three-Body Problem," *Journal of Guidance, Control, and Dynamics*, Vol. 36, No. 8, 2015, pp. 1501–1509. doi/pdf/10.2514/1.G001080

[9] Arnold, V. I., *Supplementary Chapters to the Theory of Ordinary Differential Equations*," Nauka, Moscow, 1978, p. 152.

[10] Geffroy, S., and Epenoy, R., "Optimal Low-Thrust Transfers With Constraints - Generalization of Averaging Techniques," *Acta Astronautica*, Vol. 41, No. 3, 1997, pp. 133–149. doi 10.1016/S0094-5765(97)00208-7

[11] Bonnard, B. and J.-B. Caillau. "Riemannian metric of the averaged energy minimization problem in orbital transfer with low thrust." *Annales de l'Institut Henri Poincare (C) Non Linear Analysis*, Vol. 24, No. 3. Elsevier Masson, 2007, pp. 395-411. doi:10.1016/j.anihpc.2006.03.013

[12] Kluever, C. A., and S. R. Oleson, "Direct Approach for Computing Near-Optimal Low-Thrust Earth-Orbit Transfers," *Journal of Spacecraft and Rockets*, Vol. 35, No. 4, 1998, pp. 509-515. doi:10.1016/S1000-9361(08)60121-1

[13] Gao, Y., and C. A. Kluever, "Analytic Orbital Averaging Technique for Computing Tangential-Thrust Trajectories," *Journal of guidance, control, and dynamics*, Vol. 28, No. 6, 2005, pp. 1320-1323. doi/pdf/10.2514/1.14698

[14] Mingotti, G., Topputo, F., and Bernelli-Zazzera, F., "Low-Energy, Low-Thrust Transfers to the Moon," *Celestial Mechanics and Dynamical Astronomy*, Vol. 105, No. 3, 2009, pp. 61–74. doi 10.1007/s10569-009-9220-7

[15] Betts, J., and Erb, S., "Optimal Low Thrust Trajectories to the Moon," *SIAM Journal on Applied Dynamical Systems*, Vol. 2, No. 2, 2003, pp. 144-170. doi 10.1137/S1111111102409080

[16] Topputo, F., and E. Belbruno. "Optimization of low-energy transfers," Modeling and Optimization in Space Engineering. Springer New York, 2012, pp. 389-404. doi 10.1007/978-1-4614-4469-5_16

[17] Dargent, T., "Initial And Final Boundaries Transformation When Solving Optimal Control Problem with Averaging Techniques and Application to Low Thrust Orbital Transfer," 66th International Astronautical Congress, Paper IAC-15-C1-1-4x28625, October 2015.

[18] Scharfe, D., and A. Ketsdever, "A review of high thrust, high delta-V options for microsatellite missions," 45th AIAA/ASME/SAE/ASEE Joint Propulsion Conference & Exhibit. 2009. doi/pdf/10.2514/6.2009-4824

[19] Vasiljevich, I., M. Tajmar, W. Grienauer, F. Plesescu4, N. Buldrini, J. Gonzalez del Amo, B. Carnicero-Dominguez, and M. Betto, "Development of an indium mN-FEEP thruster." 44th AIAA/ASME/SAE/ASEE Joint Propulsion Conference & Exhibit, 2008. doi/pdf/10.2514/6.2008-4534

[20] Gómez, G., Llibre, J., Martínez, R. and Simó, C. *Dynamics and Mission Design Near Libration Points, Vol. 2 Fundamentals: The Case of Triangular Libration Points*, World Scientific, Singapore, 2001, pp. 27-29.